LETTER TO THE EDITOR

Mapping the interstellar medium in galaxies with Herschel⋆/SPIRE

S.A. Eales[1], M.W.L. Smith[1], C.D. Wilson[16], G.J. Bendo[3], L. Cortese[1], M. Pohlen[1], A. Boselli[4], H.L. Gomez[1], R. Auld[1], M. Baes[2], M.J. Barlow[5], J.J. Bock[6], M. Bradford[6], V. Buat[4], N. Castro-Rodríguez[7], P. Chanial[8], S. Charlot[9], L. Ciesla[4], D.L. Clements[3], A. Cooray[10], D. Cormier[8], J.I. Davies[1], E. Dwek[11], D. Elbaz[8], M. Galametz[8], F. Galliano[8], W.K. Gear[1], J. Glenn[12], M. Griffin[1], S. Hony[8], K.G. Isaak[13], L.R. Levenson[6], N. Lu[7], S. Madden[8], B. O'Halloran[3], K. Okumura[8], S. Oliver[14], M.J. Page[15], P. Panuzzo[8], A. Papageorgiou[1], T.J. Parkin[16], I. Pérez-Fournon[7], N. Rangwala[12], E.E. Rigby[17], H. Roussel[9], A. Rykala[1], N. Sacchi[18], M. Sauvage[8], B. Schulz[19], M.R.P. Schirm[16], L. Spinoglio[18], S. Srinivasan[9], J.A. Stevens[20], M. Symeonidis[15], M. Trichas[3], M. Vaccari[21], L. Vigroux[9], H. Wozniak[22], G.S. Wright[23], and W.W. Zeilinger[24]

(Affiliations can be found after the references)

Submitted to A&A Herschel Special Issue

ABSTRACT

The standard method of mapping the interstellar medium in a galaxy, by observing the molecular gas in the CO 1-0 line and the atomic gas in the 21-cm line, is largely limited with current telescopes to galaxies in the nearby universe. In this letter, we use SPIRE observations of the galaxies M99 and M100 to explore the alternative approach of mapping the interstellar medium using the continuum emission from the dust. We have compared the methods by measuring the relationship between the star-formation rate and the surface density of gas in the galaxies using both methods. We find the two methods give relationships with a similar dispersion, confirming that observing the continuum emission from the dust is a promising method of mapping the interstellar medium in galaxies.

Key words. Galaxies: ISM – Galaxies: spiral – ISM: dust – ISM: abundances

1. Introduction

Two of the key measurements of a galaxy that are needed for any investigation of galactic evolution are the star formation rate and, because stars form out of gas, the mass of interstellar material. The standard method of measuring the gas mass is to use the 21-cm line to measure the mass of the atomic gas and the CO 1-0 line to measure the mass of the molecular material. The conversion between 21-cm flux and the mass of atomic gas is unambiguous, but the conversion factor between the CO luminosity and the mass of molecular gas (the notorious 'X factor') is uncertain both because the CO 1-0 line is optically thick and because the CO molecule is only tracing the much larger number of unseen hydrogen molecules (e.g. Bell, Viti & Williams 2007). Both techniques suffer from the problem that with current telescopes it is very difficult to measure gas masses for galaxies beyond a redshift of $\simeq 0.2$, a major limitation now that the Herschel Space Observatory (Pilbratt et al. 2010) is detecting thousands of galaxies in the high-redshift universe (e.g. Eales et al. 2010).

The idea of using the continuum emission from the dust as an alternative way of mapping the interstellar medium (ISM) has a long history, dating back at least to Hildebrand (1983). More recently, Guelin et al. (1993, 1995) and Boselli, Lequeux & Gavazzi (2002) have attempted to determine the X-factor using the continuum emission from the dust and the assumption that the gas-to-dust ratio is the same in both the atomic and molecular phase of the ISM. The problem in attempting to measure the mass of the ISM from the continuum emission of the dust is

that the conversion factors between the submillimetre flux and the mass of dust and between the dust mass and the gas mass are both poorly known. These constants have traditionally been estimated from galactic objects, such as reflection nebulae (e.g. Hildebrand 1983), but James et al. (2002) have argued that a better approach is to estimate them from the galaxies themselves, which is the approach we follow here.

In this letter, we have used both methods to map the ISM in two nearby galaxies, M99 and M100, which were two of the first targets to be observed in the Herschel Reference Survey (Boselli et al. 2010), a survey with SPIRE (Griffin et al. 2010) of 323 galaxies in a volume-limited sample of the local universe with distances between 15 and 25 Mpc. To assess the accuracy of the methods, we have used these maps to investigate the relationship between the star-formation rate in these galaxies and the density of the gas out of which the stars form. This is usually parameterised by a power-law relationship between the star-formation rate per unit volume and the gas density, $\rho_{SFR} \propto \rho_{gas}^N$ (Schmidt 1959), which for a constant scale height will result in a relationship between the star-formation rate per unit area of the disk and the surface density of the ISM which is also a power law with the same index: $\sum_{SFR} \propto (\sum_{gas})^N$. This relationship is of great interest since different theoretical models predict values of N between 0.75 and 2 (Bigiel et al. 2008 and references therein), but in this paper we are less interested in the value of N than in using the fact that there is undoubtedly some intrinsic relationship between $\sum_{SFR}$ and $\sum_{gas}$ to assess the errors, both statistical and systematic, in both methods for estimating the surface-density of the ISM.

Table 1. Fits

Method	Galaxy	N	x-residuals	y-residuals
CO/HI	M99	1.46±0.13	0.077	0.111
dust	M99	1.77±0.22	0.086	0.152
CO/HI	M100	1.38±0.08	0.070	0.096
dust	M100	1.77±0.10	0.050	0.088

2. Mapping the ISM using emission from the dust

The method of James et al. (2002) is based on the assumption that a constant fraction of metals in the ISM is incorporated in dust grains. The mass of the ISM in the galaxy is then given by:

$$M_{hydrogen} = \frac{S_\nu D^2}{\kappa_\nu B_\nu(T) Z \epsilon f} \qquad (1)$$

in which f is the ratio of the mass of metals to the mass of hydrogen in a gas with solar abundance, ϵ is the ratio of the mass of metals in the dust to the total mass of metals, Z is the metallicity of the galaxy in units of solar metallicity, and κ_ν is the mass-opacity coefficient of the dust at the frequency at which the flux has been measured. If the frequency is low enough, the Planck function reduces to the Rayleigh-Jeans approximation and the gas mass depends only linearly on the dust temperature. The importance of SPIRE is that its long-wavelength channels (350 and 500 μm) mean that it is much more likely this approximation is true than for previous space observatories such as IRAS, ISO and Spitzer.

James et al. (2002) used abundance measurements of the local ISM to estimate a value for ϵ of 0.46. We have used a value for f of 0.019 and a solar metal abundance of $12 + \log_{10}(\frac{[O]}{[H]}) = 8.69$ (Asplund et al. 2009). The dust temperature can be estimated from the spectral energy distribution of the galaxy and Z can be estimated from optical spectroscopy. The only unknowns are therefore $M_{hydrogen}$ and κ_ν, and so in principle if one has a single galaxy for which one knows the gas mass one can estimate κ_ν. On the assumption that the properties of the dust and the fraction of metals in the dust do not vary from galaxy to galaxy, one can then use this method to estimate the mass of the interstellar medium in a galaxy for which there is not a direct measurement of the gas mass.

3. The Data

M99 (NGC 4254) and M100 (NGC4321) are two spiral galaxies in the Virgo Cluster, which we take to have a distance of 16.8 Mpc. We have used the maps of the star-formation rate in these galaxies produced by Wilson et al. (2009), who combined 24-μm Spitzer images and Hα images to correct for the effect of dust obscuration, following the prescription of Calzetti et al. (2007). We have produced maps of the gas in each galaxy by combining the CO 1-0 maps of Kuno et al. (2007) and the HI maps from the VIVA survey (Chung et al. 2009). Before combining the maps, we convolved the CO map to the same resolution as the 350-μm map (FWHM of 25 arcsec). The HI map has slightly worse resolution than the 350-μm data and so we did not smooth it. In estimating the mass of molecular material from the CO 1-0 line, we have used an X factor of 2×10^{20} cm^{-2}(K km s^{-1})$^{-1}$ (Bolatto et al. 2008). In M99, the molecular material dominates the atomic gas within 80 arcsec of the galaxy centre and in M100 within 100 arcsec.

We observed M99 and M100 during the Herschel Science Demonstration Phase with SPIRE. The calibration methods and

accuracy of SPIRE are described by Swinyward et al. (2010). Images of the galaxies at the three SPIRE wavelengths (250, 350 and 500 μm) are shown in Pohlen et al. (2010). To estimate the distribution of dust temperature in each galaxy, which is necessary to estimate the surface-density of the ISM (Equation 1), we used the SPIRE images at 250 and 350 μm and the Spitzer images at 70 μm (the SPIRE image at 500 μm does not have sufficient angular resolution). We convolved the two short-wavelength maps to the resolution of the 350-μm image and re-binned the images with a pixel size of 10 arcsec. At each pixel, we fitted a single-temperature grey-body ($I_\nu \propto \nu^\beta B(\nu)$) with an emissivity index, β, of 2 to the three fluxes to estimate the dust temperature. The temperatures we derive are in the range $17 < T < 25$ K. To determine the metallicity, we used the radial profiles in Skillman et al. (1996). The remaining unknown on the right of Equation (1) is κ_ν. We estimated its value at 350 μm by scaling, using $\beta = 2$, from the value of 0.07 m^2 kg^{-1} measured at 850 μm by James et al., giving a value of 0.41 m^2 kg^{-1}. This is highly uncertain but, as we will show below, it is possible in principle to recalibrate κ_ν using the observations themselves. The flux density we used in Equation (1) was the measured 350-μm flux density. All the maps were rebinned into images with the same pixel size (10 arcsec) and astrometrically registered.

## 4. The Star-Formation Rates in M99 and M100

Figs 1 and 2 show the star-formation rate per unit area plotted against the surface density of the ISM for M99 (Fig. 1) and for M100 (Fig. 2). We have binned the images into 30-arcsec pixels before plotting these diagrams, so that the pixels are bigger than the beam size and the data for each point in the figures are clearly independent. At the distance of Virgo, a 30-arcsec pixel corresponds to 2.4 kpc. The left-hand panel in each figure shows the result from the ISM map produced from the CO and HI data, and the right-hand panel shows the result from using the ISM map produced from our alternative method.

The two panels look qualitatively very similar for both galaxies, with a tight relationship in the region of each galaxy where the ISM is dominated by molecular material (the open circles) and a much weaker relationship outside this region. There is a significant offset between the two relationships along the abscissa, which must be due to systematic errors in one or both of the methods (§5). For both methods and galaxies, we used the bisector method (Isobe et al. 1990) to fit a straight line to the points within the region dominated by molecular gas. On the assumption that there is an intrinsic relationship between the star-formation rate and the surface-density of the ISM, one way to compare the accuracy of the two methods of mapping the ISM is to compare the residuals around the best-fit lines. Table 1 shows the root-mean-square residuals of the points around each line along both the ordinate and the abcissa for both methods. Based on this criterion, mapping the ISM from the dust emission works best for M100 but mapping the ISM using the gas observations works best for M99.

There are, however, clearly systematic errors in one or both methods because the values of N determined from the two methods differ by more than expected from the errors on each value. A simple test shows that this is not necessarily the result of a problem with the dust method. We have repeated the analysis using a value for the X-factor of 1×10^{20} cm^{-2}(K km s^{-1})$^{-1}$, the value suggested by Nakai and Kuno (1995). Restricting the analysis to the region in each galaxy in which the molecular gas dominates, we find $N = 1.29 \pm 0.02$ for M99 and $N = 1.67 \pm 0.07$ for M100. The large changes show the different values of N may
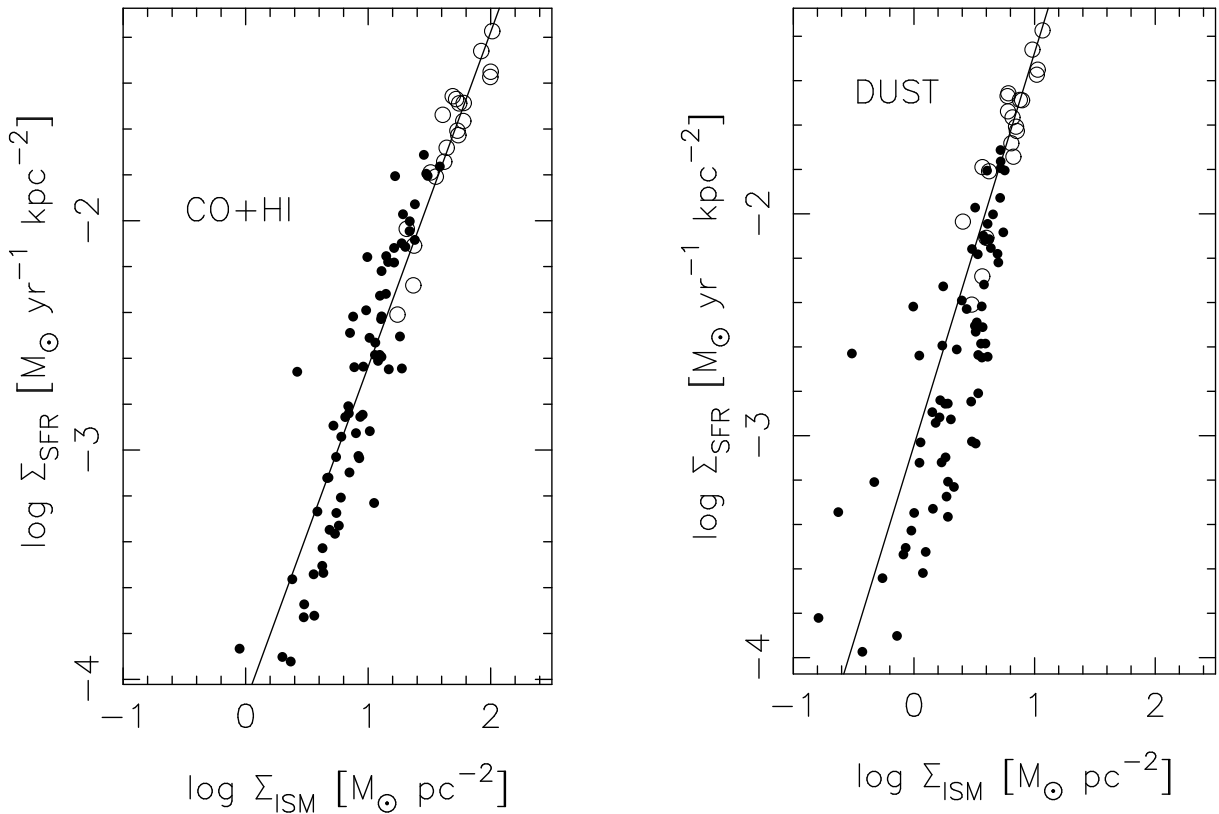
Fig. 1. The star-formation rate per unit area of the galaxy verses the surface-density of the ISM for M99. In the left-hand panel the surface-density of the ISM has been estimated from CO and HI measurements and in the right-hand panel by the method described in the text. The open circles show points within 80 arcsec of the centre of the galaxy, the region in which the surface-density of the molecular gas is greater than that of the atomic gas. The line shows a fit to the points in this region.
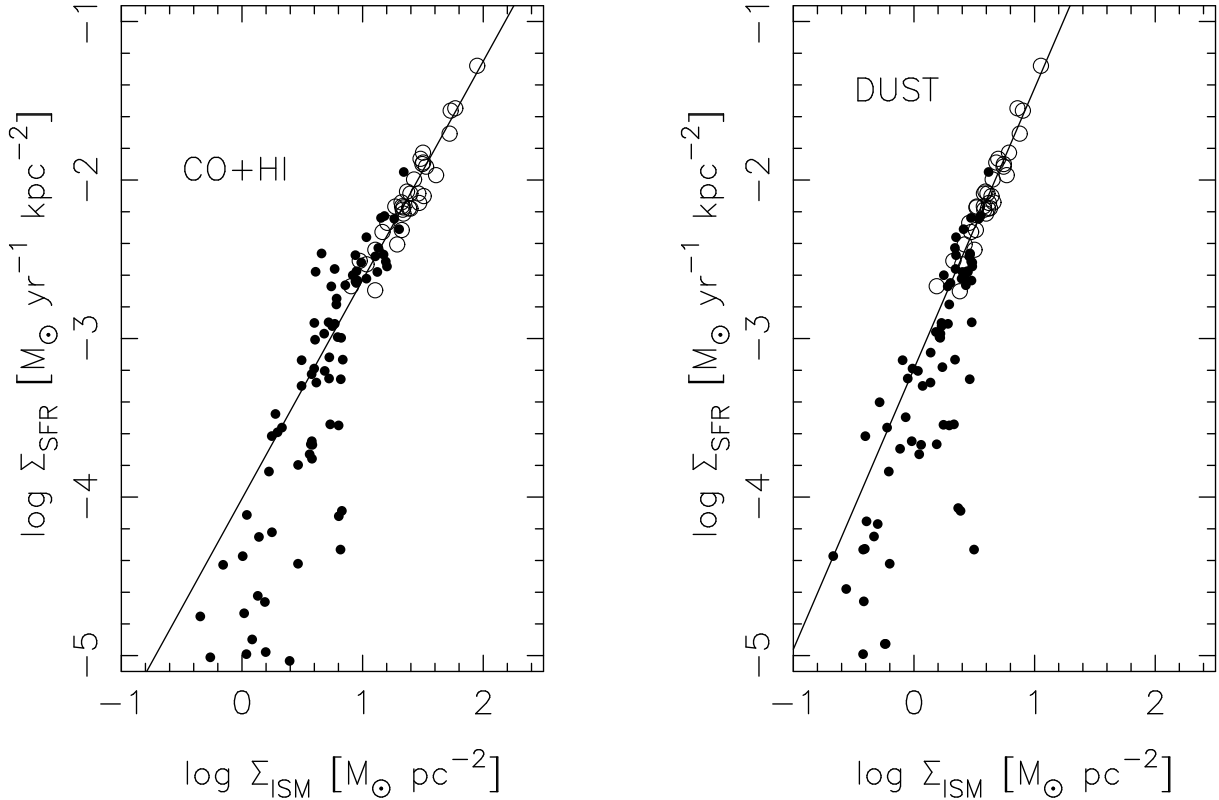
Fig. 2. The same as Figure 1 but for M100. For this galaxy the open circles show points within 100 arcsec of the centre of the galaxy, the region in which the surface-density of the molecular gas is greater than that of the atomic gas.

be as easily caused by systematic errors in the X factor as in our alternative method.

Although the focus of this paper is on testing methods for mapping the ISM in galaxies, we note that our results on the relationship between star-formation rate and the surface density agree well with recent results. Kennicutt et al. (2007) investigated this relationship within M51 and Bigiel et al. (2008) investigated it in 18 nearby galaxies. Both studies concluded that there was little relationship between star-formation rate and the surface-density of atomic gas but a strong one between the star-formation rate and the surface-density of molecular gas. This is in qualitative agreement with our finding of a strong correlation in the inner part of each galaxy, where the molecular gas is dominant. Bigiel et al. (2008) found that if one only considers the surface-density of molecular gas the value of N is $\simeq 1$. Wilson et al. (2009) used CO 3-2 observations to map the ISM in the same galaxies we have considered in this paper and found little variation in the gas depletion timescale across the disks, which implies $N \simeq 1$. Our values of N are higher than this, whichever method we use for mapping the ISM. However, if we only use the CO 1-0 observations to map the gas, we obtain $N = 1.14 \pm 0.10$ for M99 and $N = 1.02 \pm 0.08$ for M100, suggesting that it is the atomic phase of the ISM in the central parts of these galaxies which is responsible for the higher values of N.

5. Calibrating the Mass-Opacity Coefficient

We have attempted to calibrate κ_ν by requiring that the best-fit lines in the left-hand and right-hand panels of Figs 1 and 2 agree at $log \sum_{SFR} = -1.5$, a value chosen because it corresponds to the region in which the relationship between the gas surface-density and the star-formation density is tightest. We obtain a value for κ_ν at 350 μm of 0.056 m^2 kg^{-1} for M99 and 0.063 m^2 kg^{-1} for M100.

These values are three times lower than the estimate from the theoretical models of Li and Draine (2001) of $\simeq 0.19$ m^2 kg^{-1}. The only previous attempt to determine the submillimetre opacity at this wavelength directly from observations was that of Boulanger et al. (1996), who used COBE observations of dust at high galactic latitude and HI observations to obtain a relationship between submillimetre optical depth and hydrogen column density. Assuming solar metallicity and the same values of f and ϵ used in this paper (assumptions which are equivalent to assuming a gas-to-dust ratio of 153 for the high-latitude gas), we derive a value for κ_ν of 0.35 m^2 kg^{-1}, again higher than our value. Our value is also, of course, significantly lower than the value (0.41 m^2 kg^{-1}) obtained by extrapolating the measurement at 850 μm of James et al. (2002) using a dust-emissivity index of 2.

The discrepancy between our result and the James et al. result is surprising, since the method is the same in both cases, although James et al. estimated κ_ν from integrated gas and dust measurements for a large sample of galaxies whereas we have estimated it from maps of the gas and dust for individual galaxies. Since our result depends critically on the assumed value of the X factor, one way to bring the results into line would be if the values of the X factor for M99 and M100 are $\simeq 6$ times lower than the value we have assumed, which seems unlikely, however, given the recent evidence that the X factor is fairly constant between galaxies (Bolatto et al. 2008). It seems more plausible that at least part of the discrepancy is caused by our over-estimating the temperature of the dust. When fitting single-temperature models, both non-equilibrium heating of grains and the simple fact that warm dust produces more radiation than cold

dust (Eales et al. 1989) can bias the fits towards higher temperatures. The temperatures produced by our fits lie in the range $17 < T < 25$ K and the lack of any strong dependence of dust temperature on star-formation rate agrees with the recent Herschel study of the much closer galaxy M81 (Bendo et al. 2010). The temperatures are not much higher than the temperature of high-latitude galactic dust measured by Boulanger et al. (1996): 17.5 K. Nevertheless, if the temperature of the dust in both M99 and M100 were actually $\simeq 10$ K rather than 20 K, this would be enough to increase the value of κ_ν to the value expected from the James et al. study. There are other possible problems with this method, such as disagreements between different methods for measuring metallicity (Kewley & Ellison 2008) and variations in κ_ν and ϵ both within and between galaxies, but the biggest practical problem at present is the difficulty of accurately measuring the temperature of the dust. Fortunately, this should be simple to overcome by combining the Herschel observations with observations at longer wavelengths, for example at 850 μm with LABOCA and SCUBA-2.

In summary, the remarkable similarity between the right-hand and left-hand panels of Figs 1 and 2 shows that observing the continuum emission from dust is a promising method of mapping the interstellar medium in galaxies. Nevertheless, it is clear that considerable work needs to be done to calibrate this method, both in determining more accurately the temperature of the dust in individual galaxies and in determing the variation in κ_ν and the other properties of the dust in the galaxy population. The Herschel Reference Survey and the other Herschel surveys of nearby galaxies are ideal for this kind of study.

References

Asplund, M., Grevess, N., Sauval, J.A. & Scott, P. 2009, ARAA, 47, 481
Bolatto, A.D., Leroy, A.K., Rosolowsky, E., Walter, F. & Blitz, L. 2008, ApJ, 686, 948
Bell, T., Viti, S. & Williams, D. 2007, MNRAS, 378, 983
Bendo, G. et al. 2010, A&A, this volume
Bigiel, F. et al. 2008, AJ, 136, 2846
Boselli, A., Lequeux, J. & Gavazzi, G. 2002, A&A, 384, 33
Boselli, A. et al. 2010, PASP, 122, 261
Boulanger, F. et al. 1996, A&A, 312, 256
Calzetti, D. et al. 2007, ApJ, 666, 870
Chung, A., van Gorkom, J.H., Kenney, J., Crowl, H. & Vollmer, B. 2009, AJ, 138, 1741
Eales, S.A., Wynn-Williams, C.G. & Duncan, W.D. 1989, ApJ, 339, 859
Eales, S.A. et al. 2010, A & A, this volume
Griffin, G. et al. 2010, A&A, this volume
Guélin, M. et al. 1993, A&A, 279, L37
Guélin, M., Zylka, R., Mezger, P.G., Haslam, C.G.T. & Kreysa, E. 1995, A&A, 298, L29
Hildebrand, R.H. 1983, QJRAS, 24, 267
Isobe, T., Feigelson, E.D., Akritas, M.G. & Babu, G.J. 1990, ApJ, 364, 104
James, A., Dunne, L., Eales, S. & Edmunds, M. 2002, MNRAS, 335, 753
Kennicutt, R. et al. 2007, ApJ, 671, 333
Kewley, L.J. & Ellison, S.L. 2008, ApJ, 681, 1183
Kuno, N. et al. 2007, PASJ, 59, 117
Li, A. & Draine, B. 2001, ApJ, 554, 778
Pilbratt, G. et al. 2010, A&A, this volume
Pohlen, M. et a. 2010, A&A, this volume
Schmidt, M. 1959, ApJ, 129, 243
Skillman, E.D., Kennicutt, R.C., Shields, G.A. & Zaritsky, D. 1996, ApJ, 462, 147

Swinyard, B., Ade, P., Baluteau, J.-P. et al. 2010, A&A, this volume
Wilson, C. et al. 2009, ApJ, 693, 1736

[1] School of Physics and Astronomy, Cardiff University, The Parade, Cardiff, CF24 3AA, UK

[2] Sterrenkundig Observatorium, Universiteit Gent, Krijgslaan 281 S9, B-9000 Gent, Belgium

[3] Astrophysics Group, Imperial College, Blackett Laboratory, Prince Consort Road, London SW7 2AZ, UK

[4] Laboratoire d'Astrophysique de Marseille, UMR6110 CNRS, 38 rue F. Joliot-Curie, F-13388 Marseille France

[5] Dept. of Physics and Astronomy, University College London, Gower Street, London WC1E 6BT, UK

[6] Jet Propulsion Laboratory, Pasadena, CA 91109, California Institute of Technology, Pasadena, CA 91125, USA

[7] Instituto de Astrofísica de Canarias (IAC) and Departmento de Astrofísica, Universidad de la Laguna (ULL), La Laguna, Tenerife, Spain

[8] CEA, Laboratoire AIM, Irfu/SAp, Orme des Merisiers, F-91191, Gif-sur-Yvette, France

[9] Institut d'Astrophysique de Paris, UMR7095 CNRS, 98 bis Boulevard Arago, F-75014 Paris, France

[10] Dept. of Physics & Astronomy, University of California, Irvine, CA 92697, USA

[11] Observational Cosmology Lab, Code 665, NASA Goddard Space Flight Center Greenbelt, MD 20771, USA

[12] Department of Astrophysical and Planetary Sciences, CASA CB-389, University of Colorado, Boulder, CO 80309, US

[13] ESA Astrophysics Missions Division, ESTEC, PO Box 299, 2200 AG Noordwijk, The Netherlands

[14] Astronomy Centre, Department of Physics and Astronomy, University of Sussex, UK

[15] Mullard Space Science Laboratory, University College London, Holmbury St Mary, Dorking, Surrey RH5 6NT, UK

[16] Dept. of Physics & Astronomy, McMaster University, Hamilton, Ontario, L8S 4M1, Canada

[17] School of Physics & Astronomy, University of Nottingham, University Park, Nottingham NG7 2RD, UK

[18] Istituto di Fisica dello Spazio Interplanetario, INAF, Via del Fosso del Cavaliere 100, I-00133 Roma, Italy

[19] Infrared Processing and Analysis Center, California Institute of Technology, 770 South Wilson Av, Pasadena, CA 91125, USA

[20] Centre for Astrophysics Research, Science and Technology Research Centre, University of Hertfordshire, Herts AL10 9AB, UK

[21] University of Padova, Department of Astronomy, Vicolo Osservatorio 3, I-35122 Padova, Italy

[22] Observatoire Astronomique de Strasbourg, UMR 7550 Université de Strasbourg - CNRS, 11, rue de l'Université, F-67000 Strasbourg

[23] UK Astronomy Technology Center, Royal Observatory Edinburgh, Edinburgh, EH9 3HJ, UK

[24] Institut für Astronomie, Universitt Wien, Trkenschanzstr. 17, A-1180 Wien, Austria